INDIAN JOURNAL OF SCIENCE AND TECHNOLOGY

*Corresponding author.

amarppandhare@gmail.com

Development of a Novel three degree of freedom $XY\theta_Z$ Micro-Motion Stage

Rohit Navale[1], Amarsinh Kanase Patil[1], Jayesh Minase[1], Amar Pandhare[1]*

1 Department of Mechanical Engineering, Sinhgad College of Engineering, Pune, 411041, India

Abstract

Background: The piezoelectric motion with multi-degree of freedom is gaining attention in industries for modern manufacturing. High degree of positioning accuracy is obtained by complaint micro machining stages which involves high cost. A variety of stages of multi-degree motion freedom are proposed and applied for decades which can perform very high precision outputs in a wide travel range. **Methodology:** This paper mainly focuses on design, development and analysis of the 3 DOF (Degree of Freedom) XYq$_Z$ micro-motion stage. The role of each component of the stage is discussed. The various design processes are discussed and includes the discussion about the inputs to the design process as well as the constraints; both of which are dependent on the application for which the stage is used. Based on the design rules, an iterative optimization process is implemented and three design options are presented. **Findings:** The finite element modeling of all the design options are carried out. This is followed by performing deformation, static, fatigue and modal analysis on the three design options. The deformation analysis predicts that design 1 and design 2 offer a workspace of around 210 μm each along (X, Y) direction and 25 μrad along the Z direction while design 3 has deformation of 125 μm each along (X, Y) direction while 25 μrad along Z direction where as the fatigue analysis presented shows the life of around 105 cycles. Novelty: Using this technique the micro-motion stage is achieved for three degrees of freedom.

Keywords: Micro motion stage; flexure hinges; modeling; 3 degrees of freedom

1 Introduction

In micro electro-mechanical systems (MEMS) and microscope with scanning probe, alignment in optical fiber needs high-resolution motion. The ultra-high complaint positioning plays an important role in above applications. The main problem is achieving the micro/nano-positioning resolution The flexure hinges have an important advantage of no backlash, no friction loss and no need for lubrication [1]. Hence flexure hinges are finding more applications than the conventional mechanical joints. Complaint materials and flexure hinges are used in many nano/micro positioning stages. The main objective of a micro-motion stage is commonly built using a compliant mechanism and it is generally driven using a piezoelectric actuator [2]. The reason

behind the use of a compliant mechanism, which generates its motion through elastic deformation of a flexure hinge, is to replace the joints in a rigid link mechanism and, thus, avoid the use of moving and sliding parts. Further note that the use of a jointless compliant [3] mechanism to provide motion transfer, means that the problems related to wear, backlash, friction, and the need for lubrication is eliminated. This would mean that the positioning resolution, operating displacement, response time of such stage is dependent only on the actuator that drives it. Scire and many other researchers [4–8] have mentioned that if a compliant mechanism based micro-motion stage is to deliver a fast response, large displacement range, and to achieve a sub-nanometer positioning resolution, it needs to be driven using a piezoelectric actuator. The research has revealed that the extra workspace along the (X, Y) direction is to be provided. Thus, in comparison to other recently proposed designs, the 3 DOF XYq_Z Micro-motion stage presented in this study offers wider operating frequency and a larger workspace.

2 Compliant XY Motion Stage Design

A compliant mechanism [1] is a monolithic i.e. jointless mechanism that offers mechanical amplification of input signal applied. The elastic deformation in flexure elements causes motion in the complaint mechanism [9]. The amplification of the input signal is possible due to the flexible nature of the mechanism. As shown in Figure 1, the topology or the geometry of such mechanisms is of two different forms. While one of the forms is series, the other form is parallel [10]. When compared with the serial topology, the parallel form offers:

- high rigidity,
- high accuracy motion,
- light link mass, and
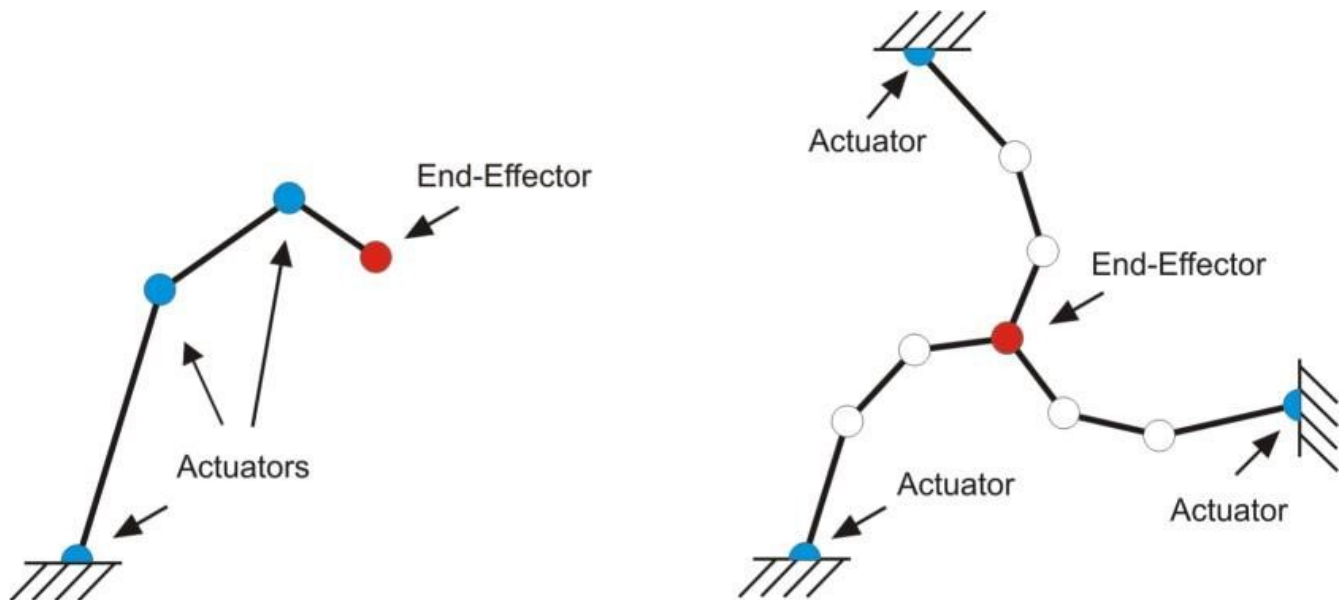- high resonant frequency

Fig 1. Schematic diagram of a serial and parallel 3-DOF mechanism: (a) serial form (b) parallel form [5,11]

Handley and Yong [5,11] have both opined that the three revolute-revolute-revolute (3RRR) geometry of a compliant mechanism is best suited in a micro-positioning application. This is because of the following advantages offered by the said geometry:

- less susceptible to kinematic variations,
- light weight,
- uncoupled stiffness between the actuators, and
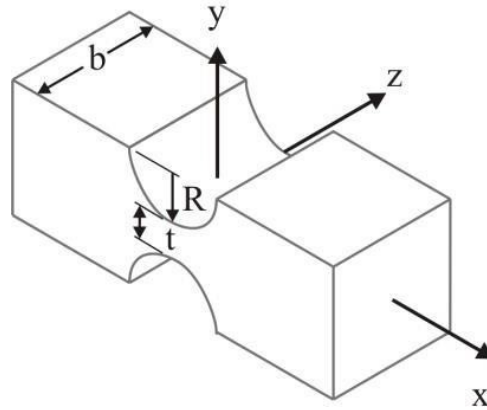- symmetrical workspace.

Fig 2. Schematic of a circular flexure hinge[11]

In Figure 2, R=radius, t =thickness, and b= width of the flexure hinge and x, y and z =axes representing degrees of freedom for the flexure hinge.

A. Flexural Hinges

A flexure hinge (refer to Figure 2) provides rotational motion between an adjacent complaint, rigid, members through bending[2]. Flexure hinge is categorized as a single axis, two axisand multiple axes (or revolute hinge). A single-axis flexure hinge, which is further sub-classified as notch type and beam type. It offers a rectangular cross-section of constant width and variable height.
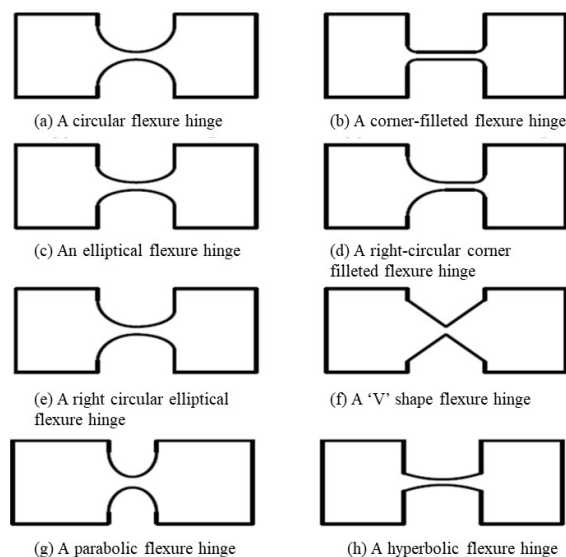

Fig 3. Design of different types of single-axis notch type flexure hinges[12]

The notch-type flexure hinges is further sub-divided into circular[2,13], corner-filleted[14], 'V' shape[12,15], elliptical right-circular elliptical[16], right-circular corner-filleted[17], parabolic and hyperbolic[18]. The design of above- mentioned single-axis notch type flexure hinges is presented in Figure 3. The single-axis notch type flexure hinges are frictionless, backlash-free and compact in design. Also besides, they are easy to fabricate and maintain. These advantages have made the single-axis notch type flexure hinges a popular choice in micro and nano-positioning applications[19].

B. Piezoelectric Actuator

The micro-motion stages are mostly actuated using piezoelectric actuators. The type of piezoelectric actuator used is stack type actuator. As shown in Figure 4, the stack type piezoelectric actuator is built using multiple wafers wired in parallel and placed mechanically in series. Each wafer is constructed from a ceramic material that is sandwiched between two electrodes. The stack type actuator generates a large amount of force as well as the displacement and most importantly its first natural frequency of resonance is very high; which makes it suitable in high frequency applications.
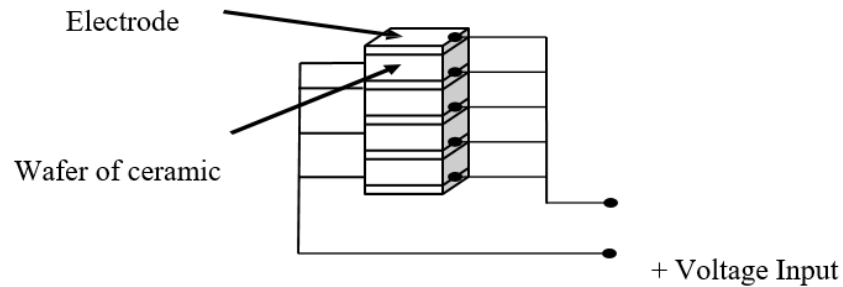
Fig 4. Construction of stack type piezoelectric actuator [20]

C. Design of Three DOF XYθ_Z Micro-motion Stage

This section presents the procedure to design the 3 DOF XYq$_Z$ micro-motion stage. Since the geometry, as well as the performance characteristics of such stage is application dependent, therefore it is necessary to first select an application that helps to define the constraints as well as the inputs required by the design procedure. Thus, any micro and nano positioning applications have been considered, this 3 DOF XYq$_Z$ micro-motion stage was designed to satisfy the demands of an application in a Scanning-Electron-Microscope (SEM) as an illustration.
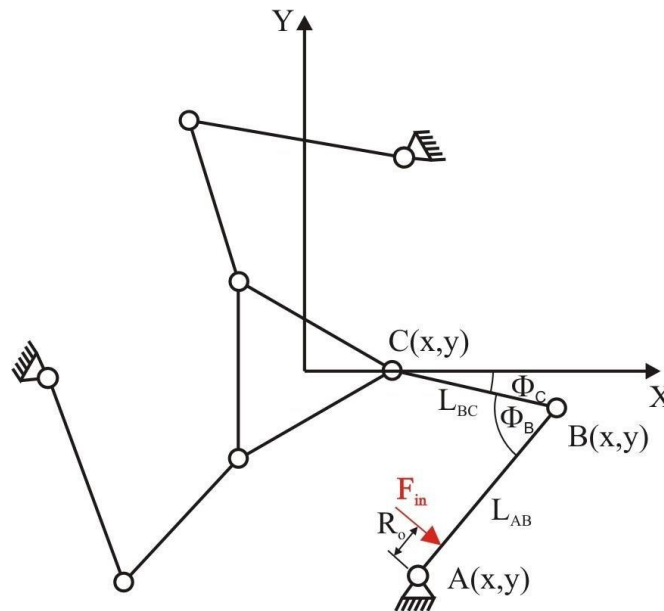
Fig 5. Schematic of linkage of 3 DOF stage along with parameters defining the linkage [11]

For the 3 DOF XYq$_Z$ micro-motion stage to fit in the sample positioner of an SEM, this stage should not be wider than 12 cm and the thickness of the stage should not be more than 2 cm.

Along the X and the Y direction, this stage should be able to offer a workspace of more than 100μm. Finally, for high speed operations, the natural frequency of the stage should be greater than 200 Hz. As mentioned before, this stage is a 3 RRR

compliant mechanism in parallel form driven using a piezoelectric stack type actuator; here after referred to as piezoelectric actuator.

The parameters defining the 3RRR parallel linkage are presented in Figure 5 , the parameters defining the geometry of the circular flexure hinge are shown in Figure 6 and the schematic for the pre-load mechanism of the piezoelectric actuator is presented in Figure 7. Also, the value of the parameters, mentioned in Figures 5 and 6 , and the material properties for the 3DOF XYq$_Z$ micro-motion stage and piezoelectric actuator are mentioned in Table 1 and Table 2 respectively.

While the value and size of the end effector, thickness of mechanism, and, length of link was deduced. The remaining values in Table 1 are deduced from the review of geometry of various linkages of 3 DOF XYq$_Z$ micro-motion stages [2,5,11,21] that offer a workspace of more than 100μm. The aforementioned information is primary to designing the stage.

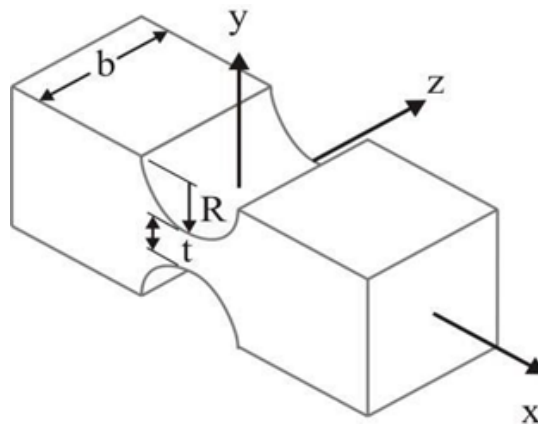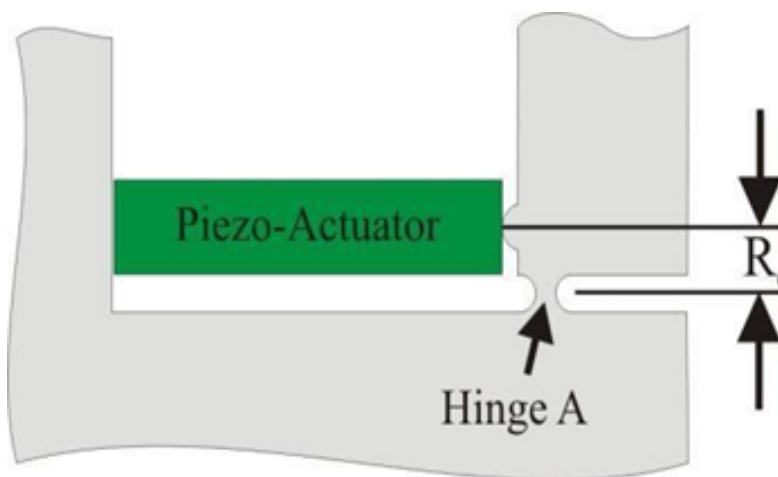**Fig 6.** Parameters defining the geometry of a circular flexure hinge [11]

Fig 7. Schematic of pre-load mechanism for piezoelectric actuator [17]

Table 1. Generic Parameter values for 3 RRR Compliant Mechanism [5,11]

3RRR Parameter	Range
End-effector size (Cx,Cy)	Fixed-Cx=20mm, Cy=0mm
Mechanism thickness (b)	Fixed - 12.8mm
Link Width (h)	Fixed - 10mm
LinkAB Length (LAB)	10 to 100 mm
LinkBC Length (LBC)	10 to 100 mm

Continued on next page

Table 1 continued

ϕB	$10°$ to $180°$
ϕC	$-100°$ to $100°$
RA, B and C	1 to 10 mm
tA, B and C	0.3 to 3 mm
Ro	2 to 10 mm

Table 2. Properties and their values of material of compliant mechanism and of piezoelectric stack type actuator [5,11]

Material Property	Value
Young's Modulus (E)	72GPa
Shear Modulus (G)	27.1GPa
Proportional limit (p)	503MPa
Actuator Property	Value
Un-loaded displacement (DLno-load) @150V	$17.4\pm2.0\mu$m
Force for zero displacement	850 N
Stiffness, Kpiezo-actuator	55N/μm
Length of actuator	20mm

D. Design Rules

Handley and Yong[5,11] have laid down a set of rules that could help when designing a compliant micro-motion stage of parallel form. These rules help in determining the values of the parameters of the linkage in Figure 5 , parameters defining the geometry of the circular flexure hinge in Figure 6 , and, parameters assisting with the design of the pre-load mechanism in Figure 7. These parameters are nothing but the design variables required by the design process. The F design rules laid down are as follows:

- To increase the workspace and $^{\theta}$Z,max, link length, L AB and L BC, is to be increased to a value that gives the maximum output.
- To increase the natural frequency ωn, link length, L AB and L BC, should be decreased, angle between the link AB and BC, ØB, is to be increased.
- To increase the workspace and rotation set ØB= 80º-90º.
- To increase the workspace, |ØC| is to be increased. On the other hand, to increase the rotation, |ØC| should be decreased. Thus, a trade-off needs to be struck to determine the optimum value of |ØC|.
- To increase the workspace and rotation Ro is to be reduced to the value that gives the maximum output. On the other hand, to increase the natural frequency ωn, Ro is to be increased. Thus, a trade-off needs to be struck to determine the optimum value of Ro. Also, while finalizing the optimum value of Ro, it is important to keep in mind the constraint posed by the piezoelectric stack type actuator in terms of its size and positioning inside the 3 DOF XYθ_Z micro-motion stage.
- The amount of rotation of the circular flexure hinge is dependent on its thickness t and hinge radius R. To ensure that the stress induced in the circular flexure hinge does not exceed the yield strength of the material, the rotation of the circular flexure hinge is not to exceed its maximum value

E. Design and FEA

Considering the design rules mentioned above, an iterative approach is implemented to find the optimum values of the parameters that define the geometry of the linkage of the 3 DOF XYθ_Z micro-motion stage. Considering the requirement of a workspace of more than 100 μm and a natural frequency of greater than 200 Hz, the final design of this stage is derived. As shown in Figure 8 below, a basic topology of this stage was first designed in Solid works. Thereafter, two more topologies were generated that were a result of the optimization to maximize the workspace as well as the natural frequency. Also, the topology was optimized to maximum strength to weight- ratio.

The stage presented in Figure 8 was analyzed using the ANSYS software. Starting with the meshing, mesh selection is an important criterion for analyzing the stage. Although different types of meshes are to be generated for a single model, not every type is suitable for the model. As far as the stage is concerned, it consists of curved regions, and, hence to capture more regions of the curve volume using a tetrahedral mesh would is to be beneficial. Using a Hex- Dominant mesh results a lack to capture the total volume resulting in inaccuracy.
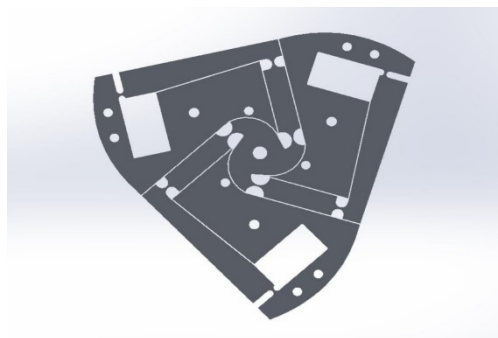
Fig 8. CAD model 1 of 3 DOF XYθ_Z Micro-motion Stage

Table 3. Value of stress and simulation conversion time for different mesh size

Mesh Size (mm)	Stress (MPa)	Conversion Time (s)
1	201.3	125
2	205.6	98
3	189.4	67
4	173.4	55
5	160.2	28

By iterating through different mesh sizes as shown in Table 3, a mesh size of 3 mm was finalized considering the time required for solution and accuracy of the results.
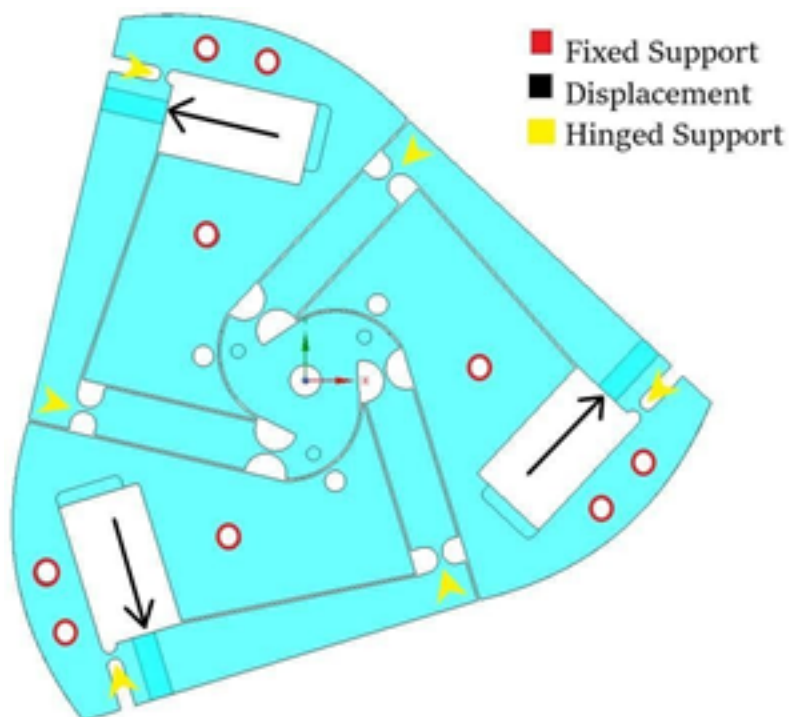

Fig 9. Free body diagram of 3 DOF XYθ_Z Micro-motion Stage (CAD model 1) showcasing the constraints (circles in red) location and direction of input (arrow in black)
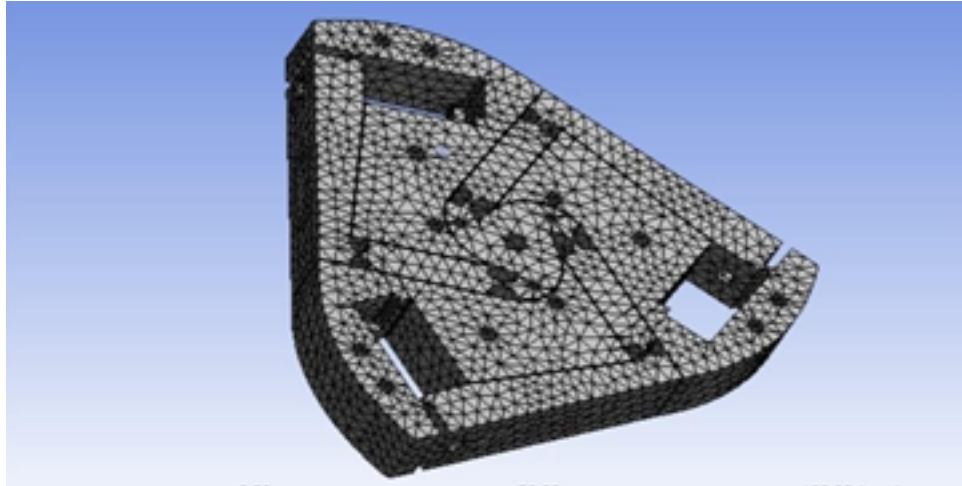
Fig 10. Meshing Of 3 DOF XYθz Micro-Motion Stage (CAD Model 1)

3 Results and discussion

A. Validation of the Numerical model

A FEA based numerical analysis is performed to investigate the workspace of a 3 DOF micro motion stage. The results presented by Handley et al. [5] and Yong and Lu [11] were compared and found in a good agreement with the results found during the present simulations,. The error in the maximum deformation was found to be less than 7%.

B. Results and discussion of numerical analysis

The numerical analysis was performed to investigate the deformation, induced stress and the life cycle of the 3 DOF micro motion stage. The results are presented below
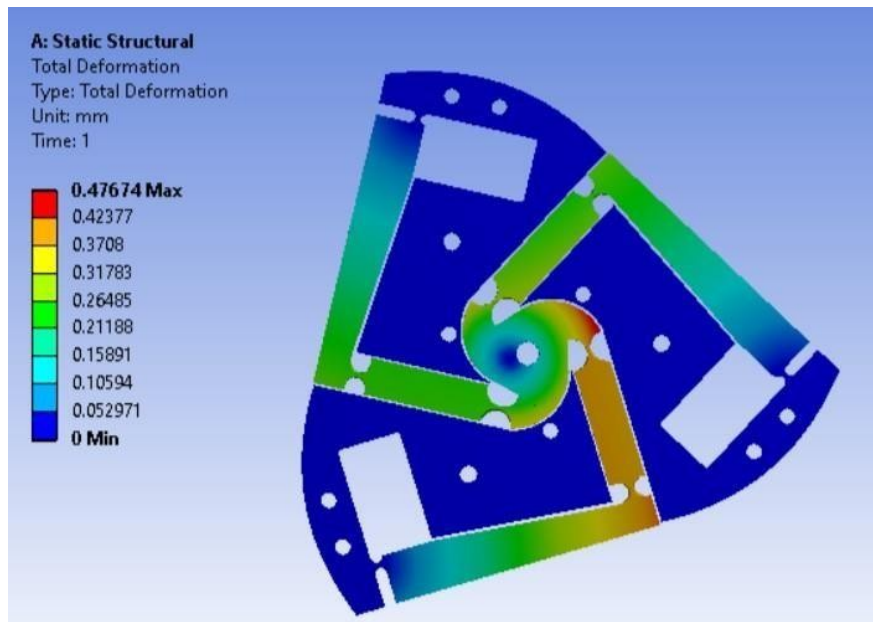

Fig 11. ANSYS output, for 850 N input, of deformation contour of 3 DOF XYθ_Z Micro- motion Stage (CAD model 1)
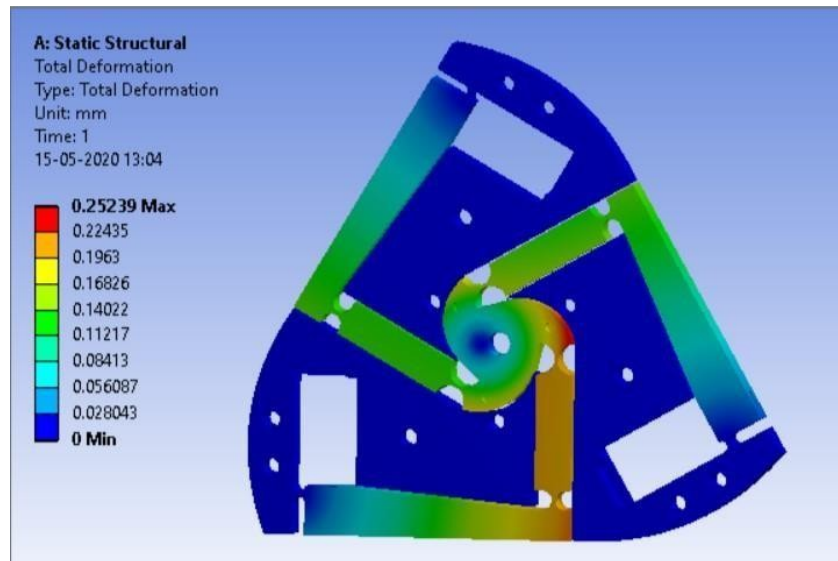
Fig 12. ANSYS output, for 425 N input, of deformation contour of 3 DOF $XY\theta_Z$ Micro- motion Stage (CAD model 1)

Figure 9 represents the free body diagram of the 3 DOF $XY\theta_Z$ Micro-motion stage. It showcases the constrain points, against which the motion of this stage is constrained. Also, Figure 9 presents the application location and the direction in which the input is applied to the linkage of this stage. As mentioned previously, this input is applied by the piezoelectric stack type actuator. The properties of this actuator are mentioned in Table 2. Figure 10 presents the meshing of the 3 DOF $XY\theta_Z$ Micro-motion stage. Based on the analysis done using ANSYS, deformation of the stage is shown in Figures 11 and 12 respectively. For an input of 850 N, the maximum deformation is found to be around 210 μm each along (X, Y) direction and 25 μrad along Z direction. Comparing Figures 11 and 12, where the input applied is 850 N and 425 N respectively, it is observed that the design of the 3 DOF $XY\theta_Z$ Micro-motion stage is linear in behavior. Also, the result of the static structural analysis of this stage is presented in Figure 13. The maximum stress induced in the circular flexure hinge is approximately 167MPa, which is below the yield strength of the material selected for manufacturing of the stage. Thus, the design of the 3 DOF $XY\theta_Z$ Micro-motion stage is safe
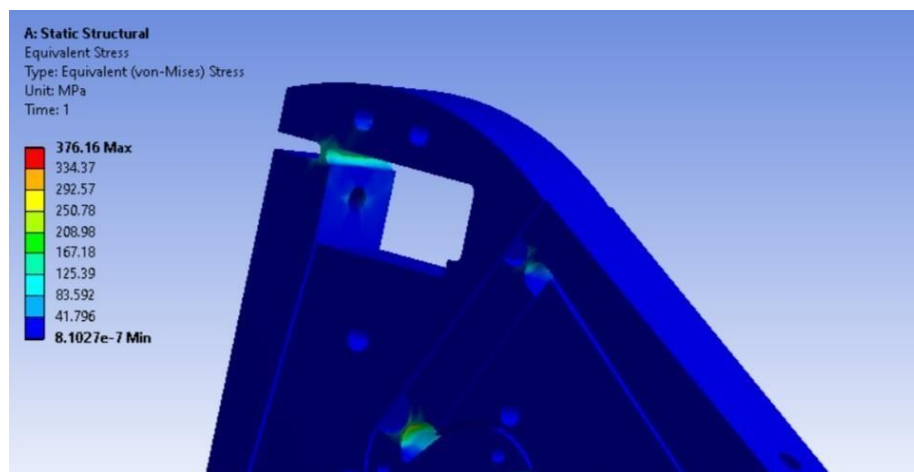

Fig 13. Stress induced in circular flexure hinge, applied with input of 850 N, based on static structural analysis of 3 DOF $XY\theta_Z$ Micro-motion Stage (CAD model 1)

In case to determine the life of the circular flexure hinge of the 3 DOF $XY\theta_Z$ Micro-motion stage, fatigue analysis is performed. The results of the fatigue analysis in Figure 14, show the circular flexure hinge has a life of approximately 10^5 cycles. To improve the fatigue life, the thickness of the circular flexure hinge needs to be increased. Doing so it reduces the workspace

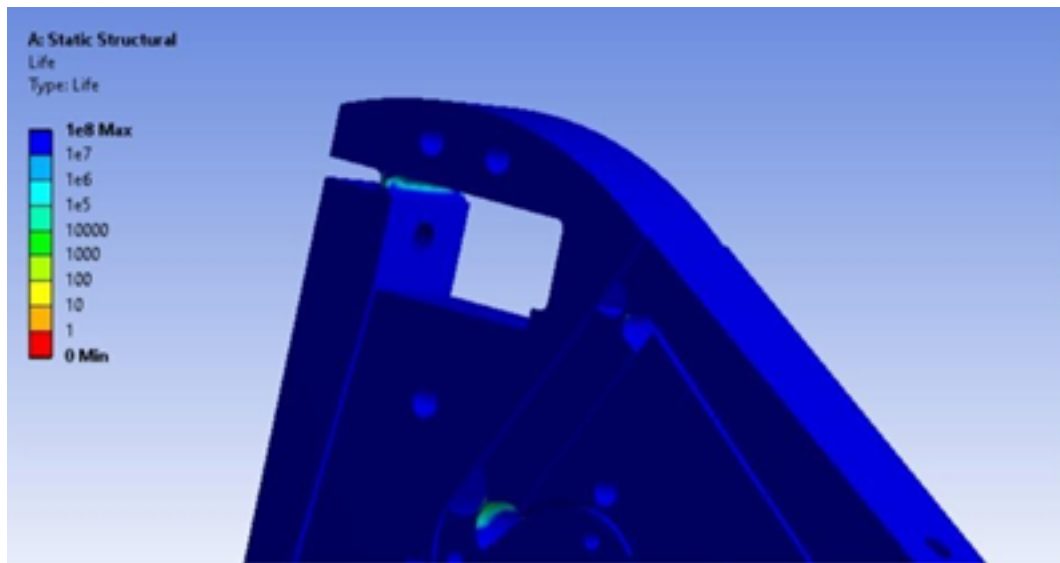reachable by the 3 DOF XYθ_Z Micro-motion stage.

Fig 14. Life of circular flexure hinge, applied with an input of 850N, based on fatigue analysis of 3 DOF XYθ_Z Micro-motion Stage (CAD model 1)
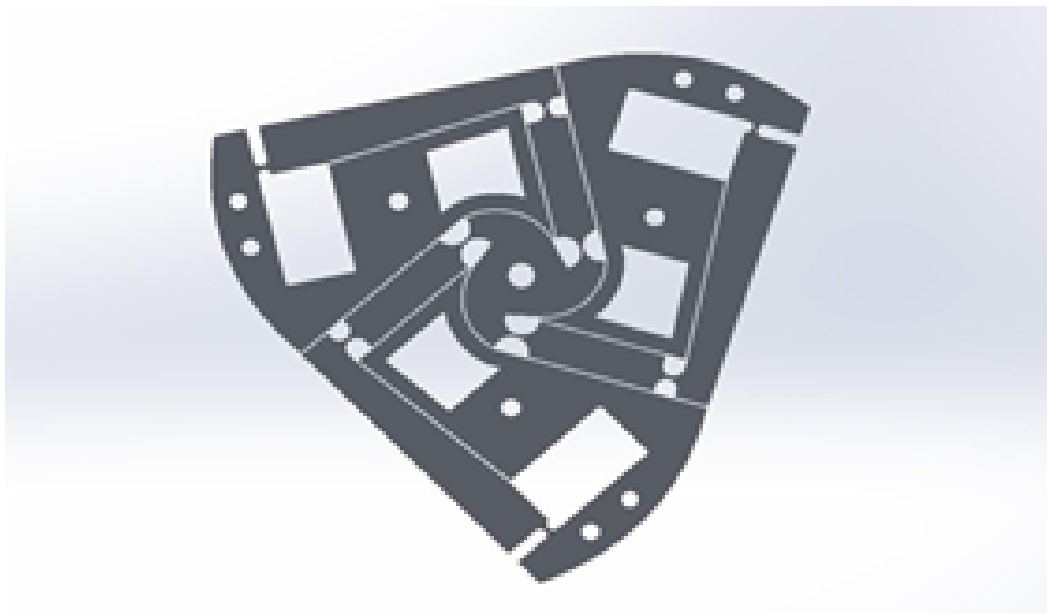

Fig 15. CAD model 2 of 3 DOF XYθZ Micro-motion Stage

In case to reduce the effective mass, the previous design of the 3 DOF XYθ_Z Micro-motion stage as represented in Figure 8 is optimized, in topology, further. A weight reduction of 10 %, when compared with the previous design in Figure 8 will lead to improvement in natural frequency of the 3 DOF XYθ_Z Micro-motion stage without hampering the strength.
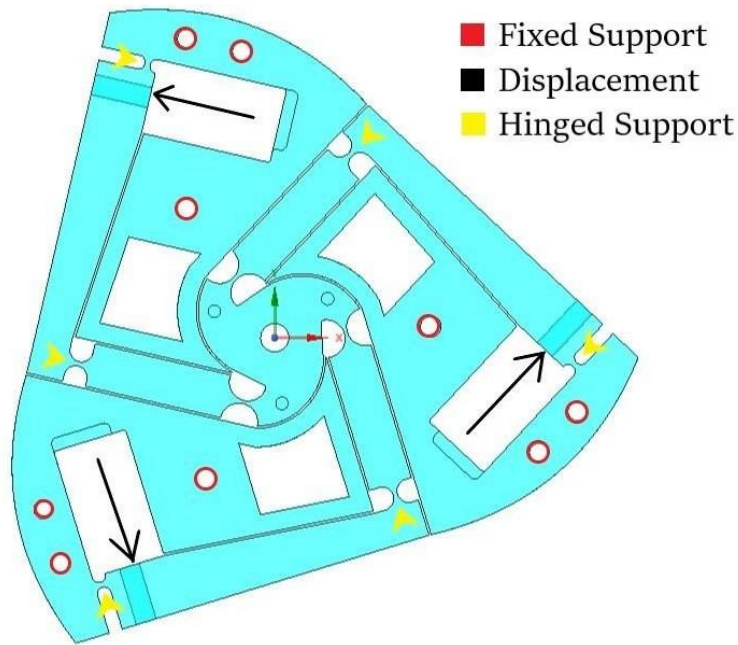
Fig 16. Free body diagram of option two design of 3 DOF $XY\theta_Z$ Micro-motion Stage (CAD model 2)
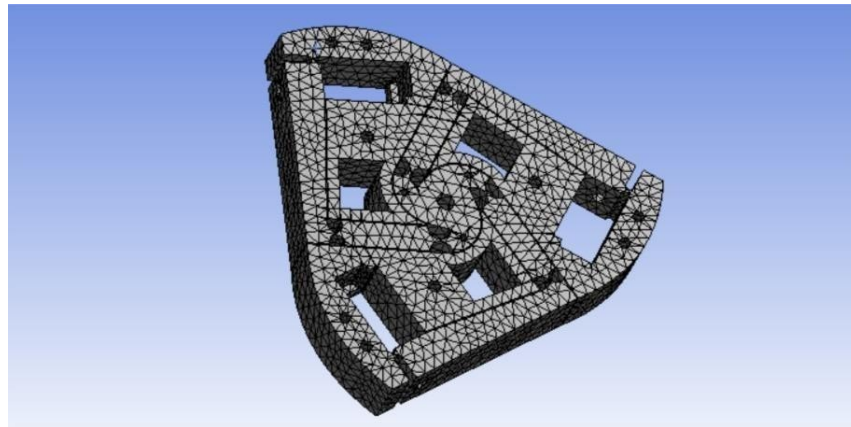

Fig 17. Meshing of 3 DOF $XY\theta_Z$ Micro-motion Stage(CAD model 2)

Figure 16 represents the free body diagram of the option two design of 3 DOF $XY\theta_Z$ Micro-motion stage. It showcases the constrain points, against which the motion of the stage is constrained. Also, Figure 16 presents the application location and the direction in which the input is applied to the linkage of the stage. As mentioned previously, this input is applied by the piezoelectric actuator. The properties of the piezoelectric actuator are mentioned in Table 2. Figure 17 presents the meshing of the option two design of 3 DOF $XY\theta_Z$ Micro-motion stage. Based on the analysis done using ANSYS, deformation of the stage is shown in Figure 18. The maximum deformation is found to around 210 μm each along (X, Y) direction and 25 μrad along Z direction.

Also, the result of the static structural analysis of the 3 DOF $XY\theta_Z$Micro-motion stage is presented in Figure 19. The maximum stress induced in the circular flexure hinge is approximately 126 MPa, which is below the yield strength of the material selected for manufacturing of the stage. Thus, the design of the stage is safe. In case to determine the life of the circular flexure hinge of the stage, fatigue analysis was performed. The results of the fatigue analysis in Figure 20 , show that the circular flexure hinge has a life of 10^5 cycle.

To improve the fatigue life, the thickness of the circular flexure hinge is needed to be increased. Doing so it reduces the workspace reachable by the 3 DOF $XY\theta_Z$ Micro-motion stage.
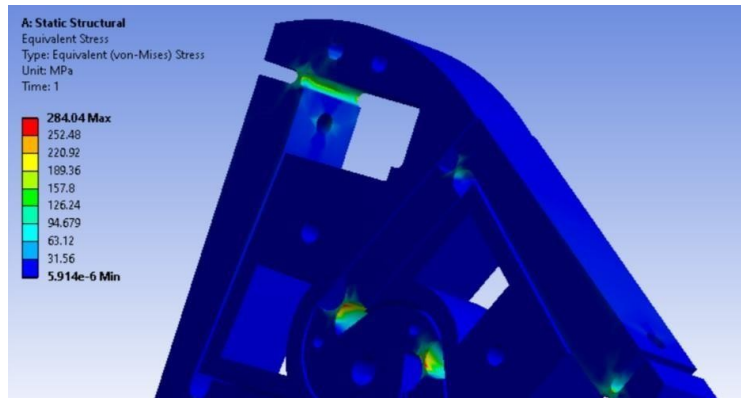

Fig 18. ANSYS output, for 850 N input, of deformation contour of 3 DOF $XY\theta_Z$ Micro- motion Stage (CAD model 2)

Fig 19. Stress induced in circular flexure hinge,for 850 N input, based on static structural analysis of design of 3 DOF $XY\theta_Z$ Micro-motion Stage (CAD model 2)

Fig 20. Life of circular flexure hinge, for 850 N input, based on fatigue analysis of 3 DOF $XY\theta_Z$ Micro-motion Stage (CAD model 2)

Option two design of 3 DOF $XY\theta_Z$ Micro-motion stage was further modified by changing the thickness of hinge to 2 mm. The modified design is presented in Figure 21.

Fig 21. CAD model 3 of 3DOF Micro-motion Stage with a hinge of 2mm thickness

Fig 22. ANSYS output, for 850 N input, of deformation contour of 3 DOF XYθ_Z Micro- motion Stage (CAD model 3)

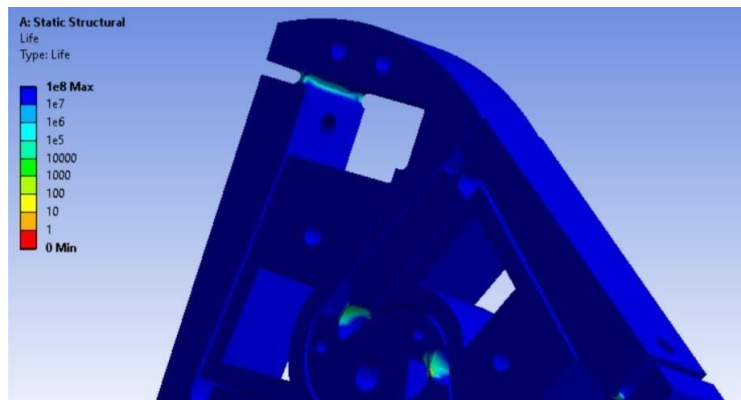**Fig 23.** ANSYS output, for 425 N input, of deformation contour of 3 DOF XYθ_Z Micro-motion Stage (CAD model 3

Fig 24. Stress induced in circular flexure hinge,for a input of 850N,based on static structural analysis of 3 DOF XYθ_Z Micro-motion Stage (CAD model 3)

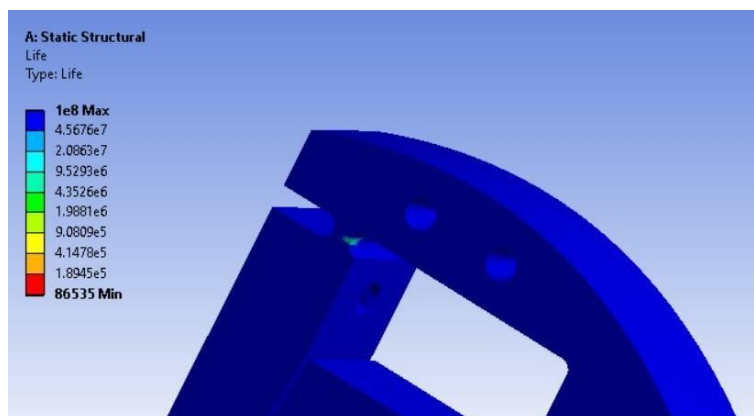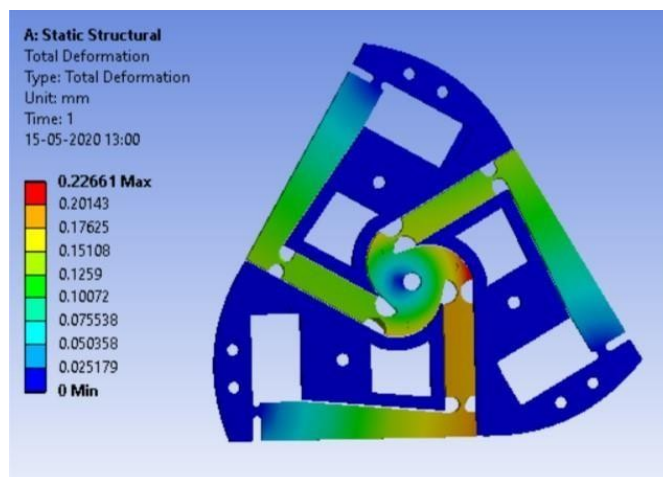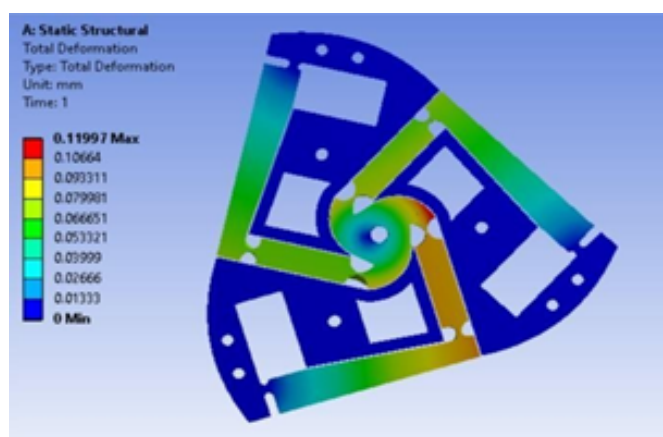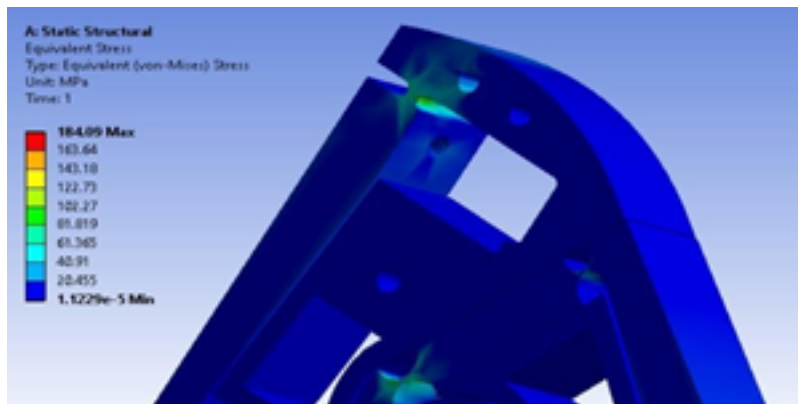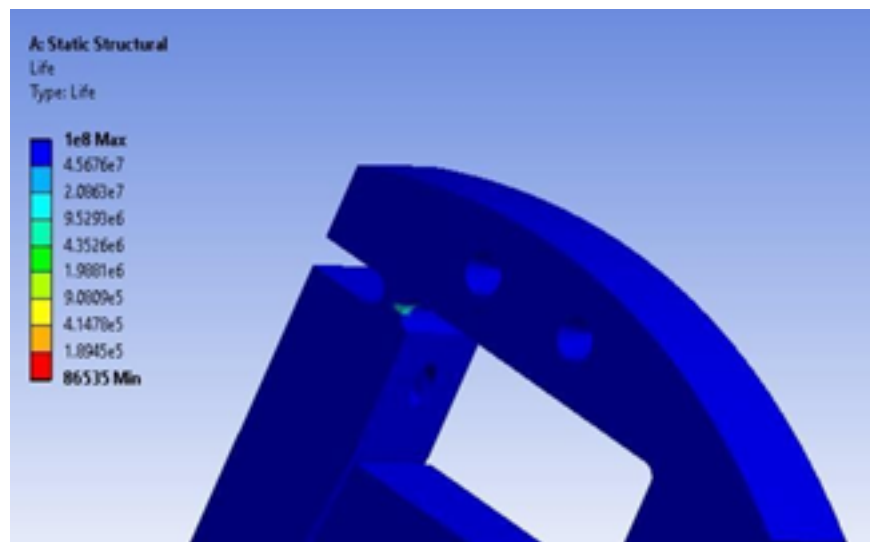**Fig 25.** Lifeof circular flexure hinge based on fatigue analysis of 3 DOF XYθ_Z Micro-motion Stage (CAD model 3)

Figure 23 shows ANSYS output, for 425 N input, of deformation contour of 3 DOF XYθ_Z Micro- motion stage. As shown in Figure 24, the maximum stress induced in the circular flexure hinge is approximately 81 MPa, which is not only below the yield strength of the material selected for manufacturing of the 3 DOF XYθ_Z Micro-motion stage but also very well below the design options presented in Figures 8 and 15. Thus, the design of the stage is safe. Similarly, an increase in the thickness of the hinge has led to an improvement in the fatigue life of the hinge. Figure 25 shows that the life of the hinge has improved to 9x10^6; a huge improvement in the fatigue life. This however comes at the expense of reduced workspace of around 125 μm each in (X, Y) direction and 25 μrad along Z direction offered by the 3 DOF XYθ_Z Micro- motion stage (refer to Figure 22).

Table 4. Comparison of designs for stress values and mass

CAD model no	Mass (grams)	Stress (MPa)	Fatigue Life (Cycles)
1	188	167.18	105
2	169.85	126.24	105
3	169.94	81.81	9x106

The aboveTable 4 illustrates a significant mass as well as stress reduction in the model achieved through optimization. A noteworthy mass reduction of around 10% is observed. Hence, the model is said to be optimized taking into account the design

and manufacturing constraints

C. Model Analysis

Modes are inherent properties of a structure and are determined by the material properties (mass, damping, and stiffness), and boundary conditions of the structure. Each mode is defined by a natural (modal or resonant) frequency, modal damping, and a mode shape. Modal analysis of the 3 DOF $XY\theta_Z$ Micro- motion stage was performed to ensure that the natural frequencies of the mechanism are not around the operating frequency, which is over 200 Hz. Based on the analysis, the results of which are presented in Figure 26, the natural frequency of the first six modes is presented in Table 5.
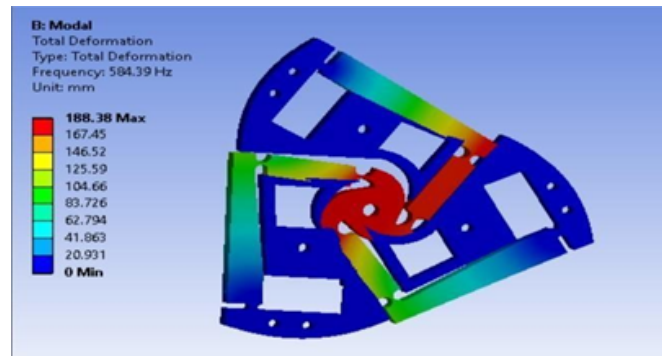

Fig 26. Mode shape of option two design of 3DOF $XY\theta_Z$ Micro-motion Stage at 584 Hz

Table 5. Mode number and modal frequencies

Mode	Frequency (Hz)
1	584.38
2	621.55
3	1181
4	1232.5
5	2233
6	2242.8

As mentioned previously, for high-speed operations, the natural frequency of the stage must be greater than 200 Hz. The results mentioned in Table 5 show that the first natural frequency of the stage is 584.38 Hz. Thus, it is to be inferred that the 3 DOF Micro-motion stage is to be utilized for high-frequency applications.

D. Comparison of Performance

The design of the 3 DOF Micro-motion stage presented in this study offers a workspace of around 210 μm each along (X, Y) direction and 25 μrad along Z direction. Also, the first natural frequency of this design is around 584 Hz, which leads to a possibility of high speed applications. When compared to other designs of 3 DOF $XY\theta_Z$ Micro-motion stage proposed recently, like the ones proposed by[8,22–27], the design presented in this study performs better both in the workspace and natural frequency.

The only recent design to perform better than the design presented in this study is the one proposed by[25], which offers 25% extra workspace along the (X, Y) direction. This extra workspace comes at the expense of lower natural frequency making the design proposed by[28] suitable for low speed operation only. Thus, in comparison to other recently proposed designs, the 3 DOF $XY\theta_Z$ Micro-motion stage presented in this study offers wider operating frequency and a larger workspace.

4 Conclusion

A 3 DOF Micro-motion stage, which is a 3 RRR compliant mechanism in parallel form driven using a piezoelectric actuator, was designed to be applied in the SEM. For the stage to fit in the sample positioner of the SEM, the dimensions of the stage were

required to be lesser than 12 cm in width and 2 cm in thickness. It was required that, along the X and the Y direction, the stage should be able to offer a workspace of more than 100 μm. Finally, for highspeed operations, it was required that the natural frequency of the stage should be greater than 200Hz.

Based on the iterative design approach, three optimizations of the 3 DOF XYθ_Z Micro-motion stage were proposed and thereafter modeled using the finite element method. Static, dynamic and deformation analysis was performed on all three design options. Finally, modal analysis was carried out to predict the natural frequencies that it is to confirm if the design of the 3 DOF XYθ_Z Micro-motion stage is used in highspeed applications. Based on the results of the analysis, following conclusions is to be drawn:

All three design options meet the requirement of workspace and natural frequency. Also, they satisfy the dimensional constraints.

Static structural analysis suggests that the stress induced is far below the maximum strength of the material used to machine the design and, thus, all three designs are safe.

Deformation analysis predicts that both design 1 and design 2 offer a workspace of around 210 μm each along (X, Y) direction and 25 μrad along the Z direction.

Fatigue analysis predicts that both design 1 and design 2 lasts a life of around 10^5 cycles. Deformation analysis predicts an increase in thickness of the flexure hinge, design 3 offers a workspace of around 125 μm each along (X, Y) direction and 25 μrad along Z direction. On a positive note, the fatigue life has improved to 9x10^6 cycles.

1. Modal analysis predicts the first natural frequency of 3 DOF Micro-motion stage to be 584 Hz thereby confirming use in high speed application.
2. In comparison to other published designs, the predicted performance of the 3 DOF XYθ_Z Micro-motion stage presented in this study is better in terms of wider operating frequency and a larger workspace.

   There is a further need to operate the stage with different frequencies. Though the details analysis has been performed for three degrees of freedom the same can be implemented for six degrees of freedom also.

References

1) Ling M, Howell LL, Cao J, Chen G. Kinetostatic and Dynamic Modeling of Flexure-Based Compliant Mechanisms: A Survey. *Applied Mechanics Reviews*. 2020;72(3). Available from: https://dx.doi.org/10.1115/1.4045679.
2) Lobontiu N, Paine JSN, Garcia E, Goldfarb M. Corner-Filleted Flexure Hinges. *Journal of Mechanical Design*. 2001;123(3):346–352. Available from: https://dx.doi.org/10.1115/1.1372190.
3) Ling M, Wang J, Wu M, Cao L, Fu B. Design and modeling of an improved bridge-type compliant mechanism with its application for hydraulic piezo-valves. *Sensors and Actuators A: Physical*. 2021;324(112687). Available from: https://dx.doi.org/10.1016/j.sna.2021.112687.
4) Scire FE, Teague EC. Piezodriven 50-μm range stage with subnanometer resolution. *Review of Scientific Instruments*. 1978;49(12):1735–1740. Available from: https://dx.doi.org/10.1063/1.1135327.
5) Handley DC, Lu TF, Yong YK, Eales C. Workspace investigation of a 3 DOF compliant micro-motion stage. *8th Int Conf Control Autom Robot Vis*. 2004;2:1279–1284. Available from: https://doi.org/10.1109/icarcv.2004.1469030.
6) Awtar S, Parmar G. Design of a Large Range XY Nanopositioning System. *Journal of Mechanisms and Robotics*. 2013;5(2):1–13. Available from: https://dx.doi.org/10.1115/1.4023874.
7) Minase J, Lu TF, Cazzolato B, Grainger S. A review, supported by experimental results, of voltage, charge and capacitor insertion method for driving piezoelectric actuators. *Precision Engineering*. 2010;34:692–700. Available from: https://dx.doi.org/10.1016/j.precisioneng.2010.03.006.
8) Gan J, Zhang X, Li H, Wu H. Full closed-loop controls of micro/nano positioning system with nonlinear hysteresis using micro-vision system. *Sensors Actuators, A Phys*. 2017;257:125–133. Available from: https://doi.org/10.1016/j.sna.2017.02.013.
9) Wu X, Lu Y, Duan X, Zhang D, Deng W. Design and DOF analysis of a novel compliant parallel mechanism for large load. *Sensors (Switzerland)*. 2019;19:1–18. Available from: https://doi.org/10.3390/s19040828.
10) Zhang S, Liu J, Ding H, Gao G. A novel compliance modeling method for compliant parallel mechanisms and its application. *Mechanism and Machine Theory*. 2021;162(104336). Available from: https://dx.doi.org/10.1016/j.mechmachtheory.2021.104336.
11) Yong YK. Kinetostatic Modelling of Compliant Micro-motion Stages with Circular Flexure Hinges. 2007.
12) Tian Y, Shirinzadeh B, Zhang D. Closed-form compliance equations of filleted V-shaped flexure hinges for compliant mechanism design. *Precision Engineering*. 2010;34(3):408–418. Available from: https://dx.doi.org/10.1016/j.precisioneng.2009.10.002.
13) Stage D, Handley DC. The Modelling and Optimal Design of a 3-DOF XYθZ Micro-Motion Stage. *Adv Cancer Res*. 2009;104:1–8.
14) Lobontiu N, Paine JSN. Design of Circular Cross-Section Corner-Filleted Flexure Hinges for Three-Dimensional Compliant Mechanisms. *Journal of Mechanical Design*. 2002;124(3):479–484. Available from: https://dx.doi.org/10.1115/1.1480022.
15) Noda NA, Takase Y. Generalized stress intensity factors of V-shaped notch in a round bar under torsion, tension, and bending. *Engineering Fracture Mechanics*. 2003;70(11):1447–1466. Available from: https://dx.doi.org/10.1016/s0013-7944(02)00115-7.
16) Chen GM, Jia JY, Li ZW. On hybrid flexure hinges. *IEEE Networking, Sens Control ICNSC2005 - Proc*. 2005;p. 700–704. Available from: https://doi.org/10.1109/icnsc.2005.1461275.
17) Chen GM, Jia JY, Li ZW. Right-Circular Corner-Filleted flexure hinges. *Proc 2005 IEEE Conf Autom Sci Eng IEEE-CASE*. 2005;p. 249–53. Available from: https://doi.org/10.1109/COASE.2005.1506777.

18) Lobontiu N, Paine JSN, O'Malley E, Samuelson M. Parabolic and hyperbolic flexure hinges: flexibility, motion precision and stress characterization based on compliance closed-form equations. *Precision Engineering*. 2002;26(2):183–192. Available from: https://dx.doi.org/10.1016/s0141-6359(01)00108-8.

19) Meng IQ. A Design Method for Flexure-Based Com- pliant Mechanisms on the Basis of Stiffness and Stress Characteristics. *Mecc e Sci Avanzate Dell ' Ing*. 2012;p. 1–110.

20) Chang SH, Tseng CK, Chien HC. An ultra-precision XYθZ piezo-micropositioner part i: Design and analysis. *IEEE Trans Ultrason Ferroelectr Freq Control*. 1999;46:897–905. Available from: https://doi.org/10.1109/58.775656.

21) Chang SH, Tseng CK, Chien HC. An ultra-precision XYθZ piezo-micropositioner part II: Experiment and performance. *IEEE Trans Ultrason Ferroelectr Freq Control*. 1999;46:906–918. Available from: https://doi.org/10.1109/58.775657.

22) Guo Z, Tian Y, Liu C, Wang F, Liu X, Shirinzadeh B, et al. Design and control methodology of a 3-DOF flexure-based mechanism for micro/nano-positioning. *Robotics and Computer-Integrated Manufacturing*. 2015;32:93–105. Available from: https://dx.doi.org/10.1016/j.rcim.2014.10.003.

23) Bhagat U, Shirinzadeh B, Clark L, Chea P, Qin Y, Tian Y. Design and analysis of a novel flexure-based 3-DOF mechanism. *Mechanism and Machine Theory*. 2014;74:173–187. Available from: https://dx.doi.org/10.1016/j.mechmachtheory.2013.12.006.

24) Clark L, Shirinzadeh B, Bhagat U, Smith J, Zhong Y. Development and control of a two DOF linear–angular precision positioning stage. *Mechatronics*. 2015;32:34–43. Available from: https://dx.doi.org/10.1016/j.mechatronics.2015.10.001.

25) Cai K, Tian Y, Wang F, Zhang D, Shirinzadeh B. Development of a piezo-driven 3-DOF stage with T-shape flexible hinge mechanism. *Robotics and Computer-Integrated Manufacturing*. 2016;37:125–138. Available from: https://dx.doi.org/10.1016/j.rcim.2015.07.004.

26) Tang C, Zhang M, Cao G. Design and testing of a novel flexure-based 3-degree-of-freedom elliptical micro/nano-positioning motion stage. *Advances in Mechanical Engineering*. 2017;9(10). Available from: https://dx.doi.org/10.1177/1687814017725248.

27) Xiao R, Shao S, Xu M, Jing Z. Design and Analysis of a Novel Piezo-Actuated XYθz Micropositioning Mechanism with Large Travel and Kinematic Decoupling. *Advances in Materials Science and Engineering*. 2019;2019:1–15. Available from: https://dx.doi.org/10.1155/2019/5461725.

28) Wang F, Liang C, Tian Y, Zhao X, Zhang D. A flexure-based kinematically decoupled micropositioning stage with a centimeter range dedicated to micro/nano manufacturing. *IEEE/ASME Trans Mechatronics*. 2016;21:1055–1065. Available from: https://doi.org/10.1109/TMECH.2015.2490803.